High Frequency Instabilities in GMR Heads Due to Metal-to-Metal Contact ESD Transients

Henry Patland, Wade A. Ogle

Integral Solutions Int'l, 2192 Bering Drive, San Jose, CA 95131

tel.: 408-941-8300, fax: 408-941-8309, e-mail: hpatland@isiguys.com; wogle@isiguys.com

Abstract **–** Utilizing a D-CDM (Direct Charged Device Model) ESD tester this study evaluates the failure rates of GMR heads by measuring high frequency instability noise events as the discrimination factor vs. ESD voltage. The D-CDM tester replicates the sub-1ns ESD event produced by metal-to-metal contact discharge that occurs as a charged component, in this case the GMR head, discharges to another object at a different electrostatic potential. By generating this ESD event at increasing charge voltages in an in-situ environment with a QuasiStatic (QST) tester, head failure effects were recorded. In addition to the standard parametrics of amplitude and resistance, advanced noise instability measurements were also performed. As is commonly understood with GMR heads amplitude may begin to fail unpredictably prior to detectable resistance failures, but this study analyzes the voltage levels where GMR heads become unstable, and their instability characteristics.

I. Introduction

Many studies have been made evaluating the failure characteristics of GMR heads vs. ESD voltages. In the past ESD events have been reproduced using Human Body Model (HBM) or Machine Model (MM) waveforms, and more recently by a method referred to as Direct Charged Device Model (D-CDM) [1]. The waveform produced by this D-CDM method approximates a high frequency, high current metal-to-metal transient between a charged device, the GMR head, and a ground potential. With this waveform a more serious ESD event can be generated, simulating worst-case conditions in an operating and handling environment.

In unison with this D-CDM module is a QuasiStatic (QST) tester. Standard measurements for the QST tester are Amplitude and Resistance. In addition a suite of high frequency instability measurements supported by the QST Tester were enabled, including Maximum Amplitude Noise (MAN) and Popcorn/ACField, and in the event of a 'noisy' result the high frequency head readback signal was digitized.

With this test configuration the voltage levels where GMR head become unstable, and the characteristics of this instability, was analyzed.

II. Measurement Equipment

Two components were used to perform this measurement. The D-CDM Stress Tester with EPS-100 Power Supply and the QST-2002 with optional AC Measurement Channel, both produced by Integral Solutions Int'l (ISI). The fundamentals of the AC Measurement Channel in context with the means of detecting high frequency GMR instabilities is discussed below.

II.a. D-CDM ESD Transient

The D-CDM ESD Transient was produced using the ISI D-CDM Stress Tester. This tester incorporates a bipolar programmable voltage source for charging the GMR to a desired charge voltage, then a circuitry to rapidly discharge the GMR, resulting in an ESD event replicating that of a metal-to-metal CDM discharge. After this discharge operation the D-CDM Module disconnects the charge circuit from the head in order to support measurements by an external device. In this study the D-CDM unit was connected to the ISI QST-2002 with AC Channel Option, in order to perform post-ESD QST measurements.

Figure 1 shows the waveform produced by the D-CDM device. The waveforms shown are with a 5pF

Disk Capacitor installed, with an applied charge voltage of 10V and 1V respectively.

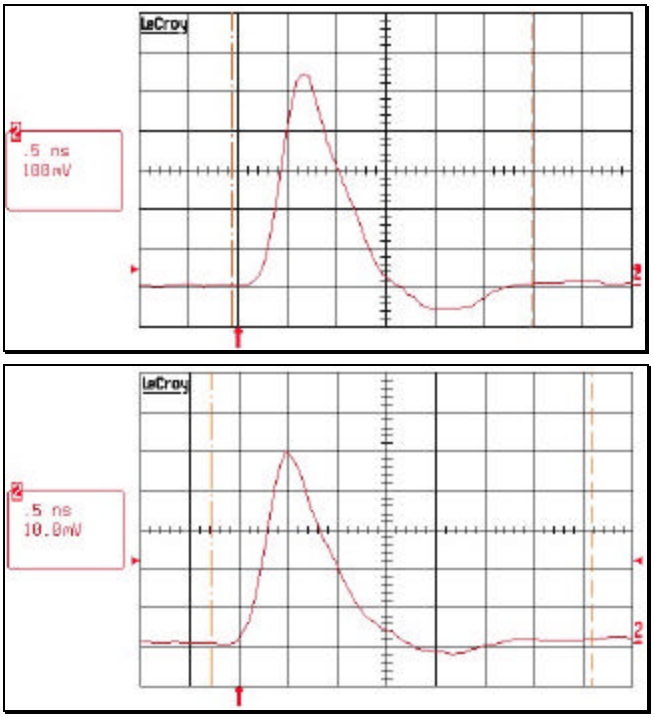

Figure 1: D-CDM Waveforms produced with a +1V and 10V charge voltage and 5pF Disk Capacitor.

II.b. High Frequency Instability Measurement – Maximum Amplitude Noise (MAN)

The ISI QST-2002 with AC Channel Option supports an integrated test called Maximum Amplitude Noise, which can be enabled together with Resistance and Amplitude as part of an ESD sweep. The algorithm of this test is to sweep through a range of DC magnetic fields, and at each field measuring both the peak and RMS noise detected at this field. This test closely correlates with Barkhausen Hard and Soft Kinks detected on the Transfer Curve, but is much more accurate in detection in that a high-frequency measurement channel is used. [2]

Barkhausen Kinks have been typically characterized as an instability in GMR performance at a certain range of magnetic fields. This instability is presented on the Transfer Curve as a DC delta in resistance at a certain range of magnetic fields. In actuality the GMR is rapidly toggling between two (or perhaps more) 'stable' resistance states, but the nature of the relatively low bandwidth of the Transfer Curve measurement channel precludes this from being easily quantified as part of this measurement. This is especially true if the instability occurs through a relatively wide, example 10Oe, range of magnetic fields, which appear distrorted when measured through a low bandwidth channel. Figure 2 shows an example of a GMR head with both a hard and a soft kink.

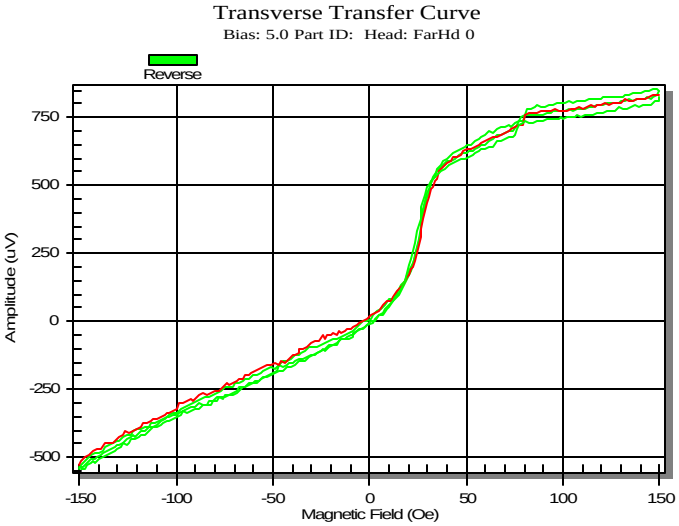

Figure 2: GMR Head with a Soft Kink located around +25Oe and Hard King at around +80Oe.

The MAN test utilizes an AC Measurement Channel which can easily quantify these instabilities, and present them as both Peak Amplitude and RMS Amplitude vs. applied Magnetic Field. For the purpose of this study the maximum value of these results were measured vs. applied ESD, independent of where the 'unstable' magnetic field location occurred, in order to present the data as a worst-case instability occurance.

Figure 3 shows an example of a MAN test result on the same GMR head shown in Figure 2. The Peak Noise level vs. Magnetic Field is shown as the Max Noise Amp curve, and the RMS Noise level is shown as the Noise Amp curve. As described the maximum value of these two curves would be presented on the ESD Sweep plot, which in this case would be ~77uV maximum Peak Noise and ~54uV maximum RMS noise.

During the ESD sweep, once an instability was detected at a certain magnetic field using the MAN test that field was applied and the resulting AC readback channel digitized, using the integrated digital scope feature on the ISI QST-2002. A typical example of a digitized sample taken at a 'noise-free' magnetic field is shown in Figure 4, whereas Figure 5 shows the same head but while the 'noisy' DC magnetic field is applied.

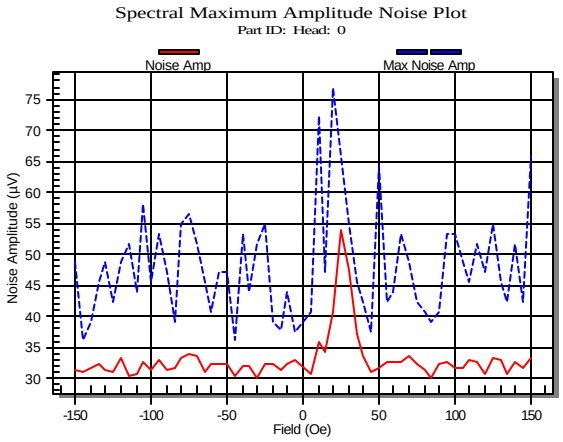

Figure 3: MAN Test result of same GMR Head represented in Figure 2: with maximum Peak Noise of ~77uV and maximum RMS Noise of ~54uV, both occurring near +25Oe.

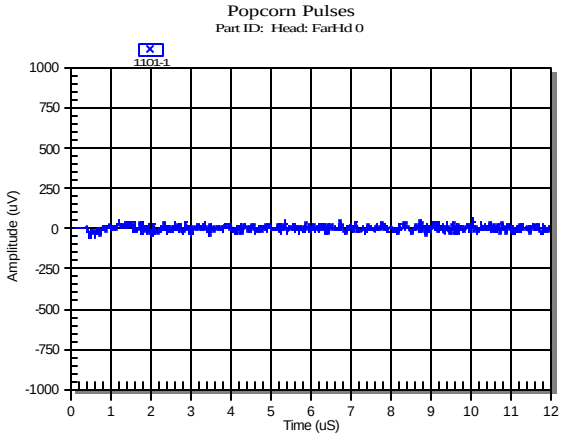

Figure 4: Digitized sample through an AC measurement channel of a GMR Head at a 'noise-free' DC magnetic field (baseline).

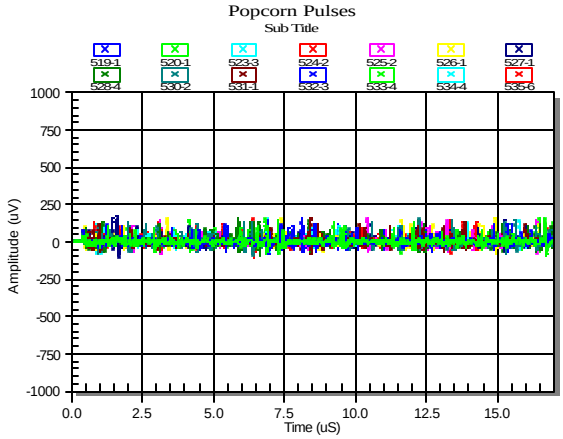

Figure 5: Digitized sample through an AC measurement channel of a GMR Head at a 'noisy' DC magnetic field.

II.c. High Frequency Instability Measurement – Popcorn Noise with Magnetic Field Excitation (Popcorn/ACField)

In addition to MAN, Resistance, and Amplitude, during the D-CDM ESD sweep the Popcorn Noise Test with AC Magnetic Field excitation was enabled. This measurement utilizes the same AC channel measurement concept as the MAN Test, but produces a pure count of noise pulses detected above a certain Threshold. While the measurement threshold is somewhat arbitrary, a threshold suitably higher than the baseline noise level must be used. During this measurement both write excitations and field excitations were simultaneously performed, in order to characterize noise detected from both field- and write-induced sources.

While field-induced noise detected during this measurement should correlate closely with the MAN test results, the goal was to see if additional noise would be detected from write-induced effects. This can be characterized by monitoring if additional Popcorn/ACField counts were detected at D-CDM voltages where there was no detectable MAN noise. Similarly, by analyzing the digitized data and evaluating the location in time of the detected noise pulse with respect to the end of the write operation, the counts could be categorized as being field- or write-induced.

Figures 4 and 5 above were taken from the Popcorn/ACField measurement. While digitization of error events was enabled, the parametric result for this study was simply the total number of counts detected, as detected above a defined threshold over a certain number of test repetitions while simultaneously applying a single period of an AC magnetic field.

III. Measurement Parameters

With typical GMR heads failing at a D-CDM voltage of around 5V, the sweep range of the D-CDM pulses was chosen to be 1V-7V, with a coarser increment (either 0.5V or 1V) up to 3V and a finer increment (0.2V) from 3V to 7V. Both ESD pulse polarities were chosen, such that at each desired charge voltage the measurement would be repeated for both a positive and a negative polarity ESD event.

The measurements after each ESD event were Amplitude, Resistance, Popcorn/ACField count, MAN Peak Noise, and MAN RMS noise, where the

MAN results are the peak levels detected across the range of magnetic fields. The magnetic field range chosen for all measurements, other than Resistance, was +- 150Oe. For the Amplitude result the Peak-to-Peak Amplitude at +-100Oe was extracted from the +-150Oe field sweep, and this was reported as the Amplitude result.

For the Popcorn/ACField test parameters the number of noise pulses counted was with 1497 iterations, Write Current 45mA, Write Frequency 150Mhz, Threshold 100uV, and timing was Write 50uS, Delay 2uS, and Read 15uS. With the ACField mode enabled, simultaneously during the 1497 iterations one full period of triangle-wave magnetic field with peak values +-150Oe was applied.

IV. HGAs Utilized

Ten GMR HGAs were utilized for this measurement. All ten were from the same manufacturer, designed for areal density of about 25Gbit/in^2. The material composition of these HGAs were CoFe/NiFe free layer, synthetic pinned layer, with antiferromagnetic layer of PtMn.

Prior to the application of ESD Stress all ten were characterized for initial performance. All ten had reasonable resistance and peak-to-peak amplitudes, and little or no detectable Popcorn/ACField counts. Of these nine had low initial MAN noise, whereas one had detectably high initial MAN noise. This HGA will be discussed separately, as the results showed an interesting trend that may require further investigation in a separate study (referred to as Head #7 below).

V. Measurement Results

Figure 6 shows a typical result from the D-CDM ESD Sweep analysis. At increasing D-CDM charge voltage values both Positive and Negative ESD events were performed, so the parametric measurements were repeated for each polarity of ESD. In decending order on the plot the results of Amplitude, Resistance, Popcorn/ACField, MAN maximum RMS Noise, and MAN maximum Peak Noise are displayed.

Figure 7 shows a typical MAN test result after application of one of the 'noisier' D-CDM ESD transients (specifically after a –3.2V, ie Negative, D-CDM ESD event). In this instance the maximum Peak Noise is at 85Oe, with a value of ~130uV. Comparatively RMS Noise had a maximum value of ~55uV at 140Oe. On Figure 6 these values can be seen in the Negative Sweep result at 3.2V D-CDM voltage.

The following Figures 8-17 show the D-CDM ESD Profile Plots for all 10 subjected HGAs. Heads #1-#7 show significant instabilities detected during the ESD sweep, while Heads #8-#10 did not.

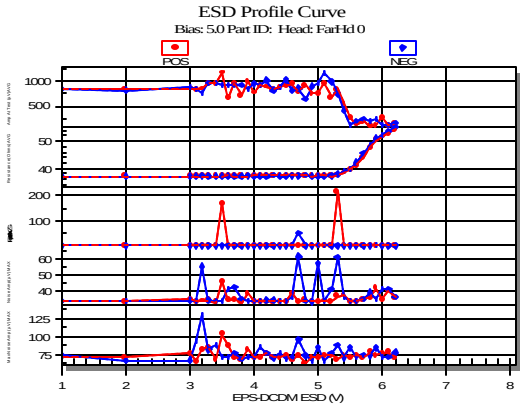

Figure 6: D-CDM ESD Profile Plot, with parametrics vs. increasing D-CDM ESD bipolar (Pos and Neg) charge voltage. From top to bottom parametrics are Amplitude, Resistance, Popcorn/ACField, MAN maximum RMS Noise, and MAN maximum Peak Noise.

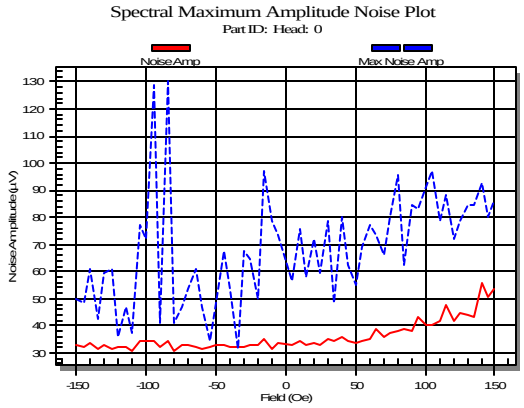

Figure 7: MAN Test result after D-CDM ESD event of –3.2V, with maximum Peak Noise of ~130uV and maximum RMS Noise of ~55uV.

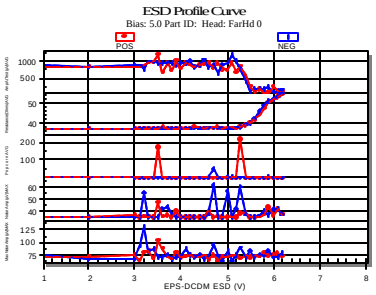

Figure 8: D-CDM ESD Profile Plot, Head #1.

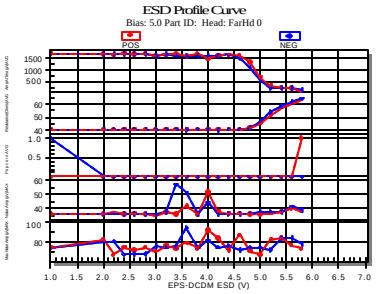

Figure 9: D-CDM ESD Profile Plot, Head #2.

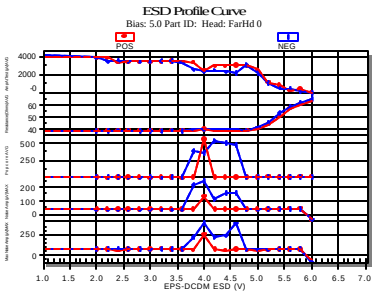

Figure 10: D-CDM ESD Profile Plot, Head #3.

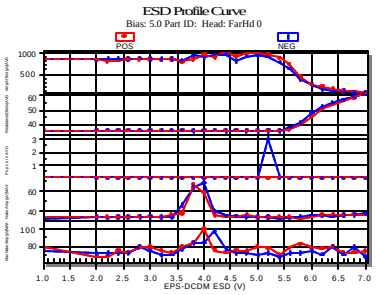

Figure 11: D-CDM ESD Profile Plot, Head #4.

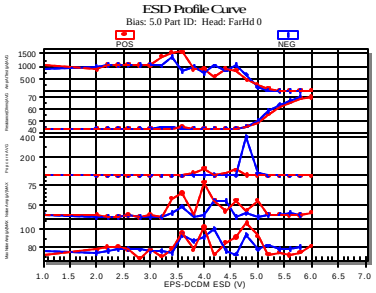

Figure 12: D-CDM ESD Profile Plot, Head #5.

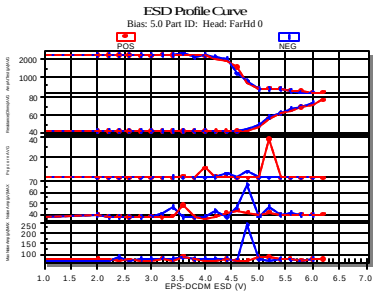

Figure 13: D-CDM ESD Profile Plot, Head #6.

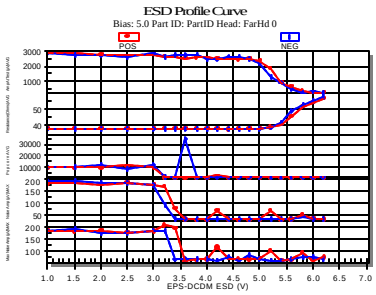

Figure 14: D-CDM ESD Profile Plot, Head #7.

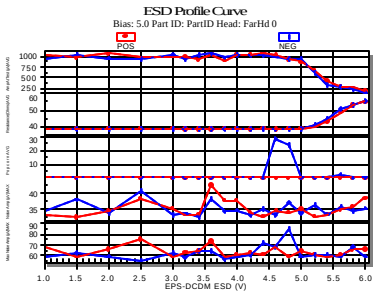

Figure 15: D-CDM ESD Profile Plot, Head #8.

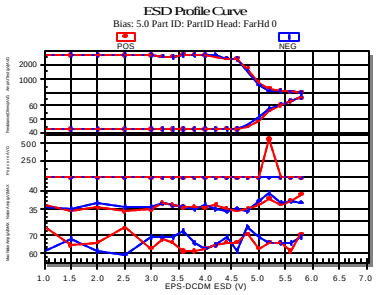

Figure 16: D-CDM ESD Profile Plot, Head #9.

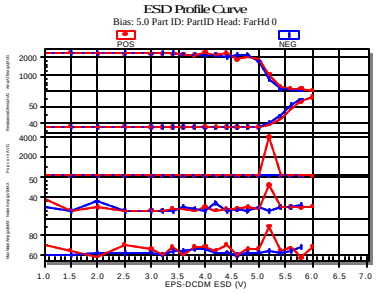

Figure 17: D-CDM ESD Profile Plot, Head #10.

VI. Measurement Data Analysis; Effects of D-CDM ESD on GMR Heads

In analyzing the results of the D-CDM ESD Sweep data the following observations were seen.

7 out of 10 of the HGAs tested demonstrated high instabilities prior to resistance failure, whereas the other 3 were more tolerant. On these 7 HGAs, the D-CDM ESD voltage where instabilities were initially detected averaged about 25% lower than resistance failure voltages (instabilities occurred on average at about 3.6V, whereas initial resistance failure occurred on average at about 5V).

In about half the cases the ESD voltages where high frequency instabilities occurred was synchronous with the Amplitude variation vs ESD. Correspondingly, in the other half of cases instabilities were detected while amplitude remained stable. In all cases consistent amplitude degradation occurred long after any initial detection of instability, approximately 0.1-0.2V prior to resistance degradation.

By analyzing the resulting Transfer Curve data from these sweeps, it was identified that hard and soft kinks, although often times very subtle, were the primary source of instability. Dependent on the field location(s) of the kink(s) it may or may not directly affect amplitude, but always appeared in the high frequency instability measurements. This was why high frequency instabilities only generally tracked with amplitude variations.

Figures 18 - 19 demonstrate this phenomenon, where Figure 18 is the Transfer Curve of one head at an ESD voltage prior to the detection of high frequency instability, whereas Figure 19 is after instability has occurred due to a larger ESD voltage. Note that the reported amplitudes between the two measurements correlate well, showing little amplitude difference, even though the latter curve is obviously 'noisy'.

Additionally, in further analyzing Head #7, the initial MAN noise prior to ESD was caused by a soft kink near +100Oe. This kink was continuously visible as ESD voltages approached 3.5V, but above this voltage the effects of this kink seemed to 'disappear' from the ESD sweep data. In actuality because the kink was close to the edge of the +-150Oe field sweep the kink was just shifted outside of our measured field range as a result of the ESD event.

Figures 20-21 show the initial soft kink on head #7, at ESD voltages lower than 3.5V. Figures 22-23 show the results of this head at 3.5V ESD, where the kink has begun to shift. Figures 24-25 show the results of this head at about 4V ESD, where the kink has shifted completely outside the measurement range.

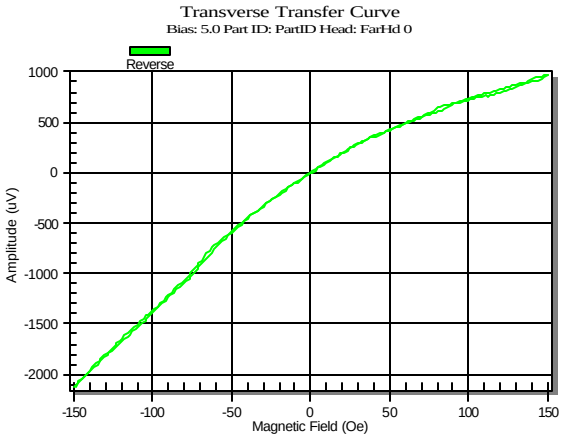

Figure 18: Transfer Curve of a head at ESD voltages below the detection of high frequency instability.

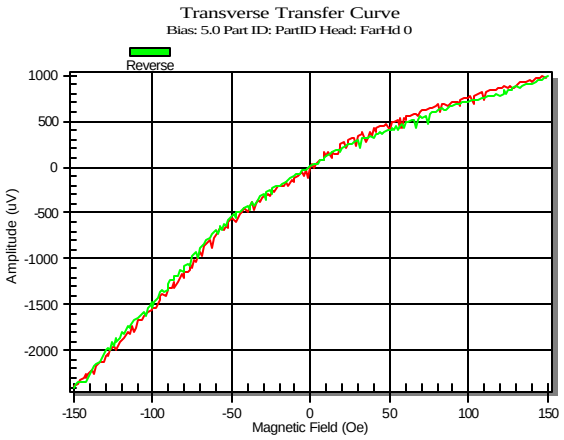

Figure 19: Transfer Curve of the same head at ESD voltages where high frequency instability is occurring.

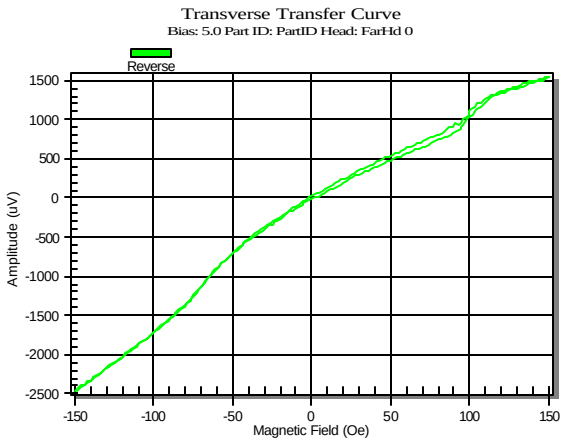

Figure 20: Typical Transfer Curve of Head #7 at ESD voltages below the 3.5V ESD voltage level, with a soft kink near +100Oe.

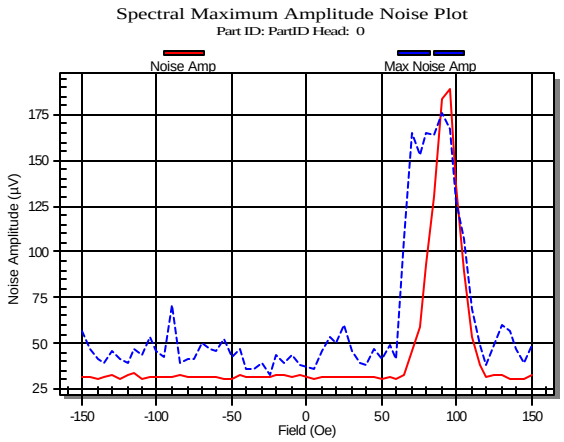

Figure 21: MAN Test result corresponding to Transfer Curve from Figure 20, with corresponding high noise at +100Oe.

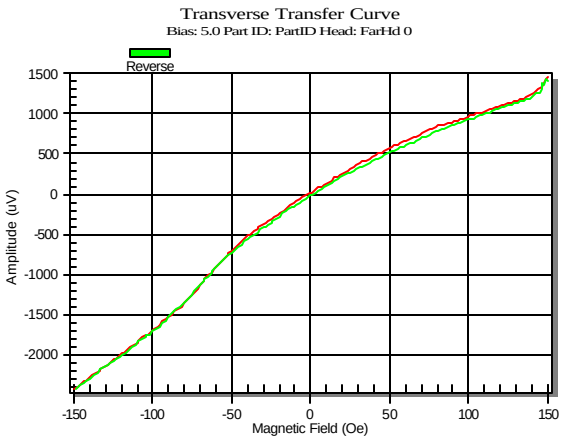

Figure 22: Transfer Curve of Head #7 at 3.5V ESD Voltage. Notice shift of soft kink to +150Oe.

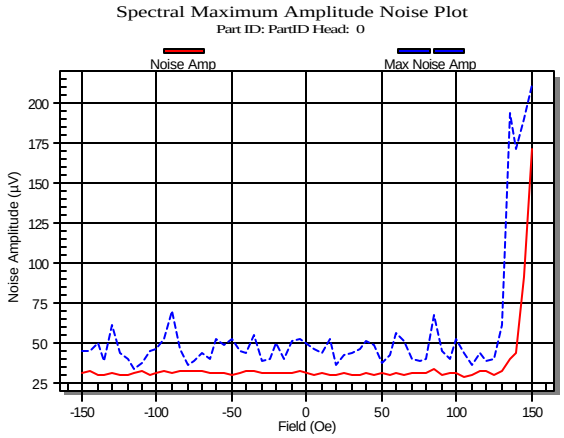

Figure 23: MAN Test result corresponding to Transfer Curve from Figure 22, with corresponding high noise shifted to +150Oe.

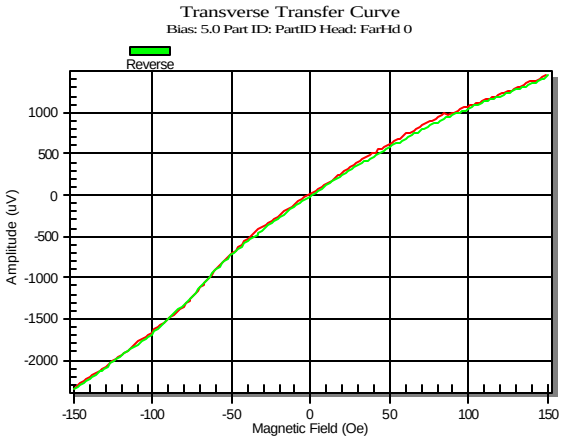

Figure 24: Transfer Curve of Head #7 at about 4V ESD Voltage, with no detectable soft kink.

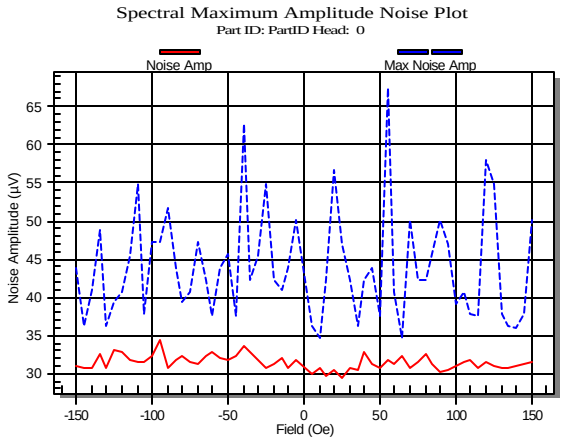

Figure 25: MAN Test result corresponding to Transfer Curve from Figure 24, with no detectable soft kink noise.

This 3.5V ESD level on Head #7 correlates well with the voltage at which most of the other heads became unstable. Based on this it can be assumed that while the overall effects were different the root cause, that being a change in magnetics on these HGAs due to a ~3.5V D-CDM ESD event, is the same.

In all cases no additional instabilities could be detected from write-induced effects, based on the relationship between the Popcorn/ACField results vs. either of the MAN test results.

In general D-CDM ESD Polarity played little role in the ESD Profile Curve, as each polarity produced similar results.

VII. QST Amplitude as a Valid ESD Characterization Parametric

While QST amplitude variation has shown to be a useful parametric for quantifying ESD effects in the past, this can be prone to error as it may miss certain notable conditions, specifically hard and soft kinks. From this set of data it appeared that these kinks were the largest instability factor produced by ESD, and in approximately 50% of the cases the amplitude measurement was unsuccessful at detecting this condition.

In a general production environment QST amplitude will be even weaker in detecting this condition. While it is easy to empirically analyze amplitude stability during an ESD sweep, it is a different story altogether when attempting to characterize head performance without the benefit of this sweep data. Assume a head has been subjected to partial ESD damage, then an amplitude measurement is performed in an effort to detect this damage. Without the luxury of relative data prior to and after this ESD damage it would be difficult to gather useful data from amplitude alone. Measurements such as MAN, or perhaps Barkhausen Jump and/or highly-repetitive amplitude readings with high enough sensitivity, appear much better at detecting these failure conditions.

VIII. Summary

Based on this data, we can conclude that D-CDM ESD did have a significant affect on these HGAs near 3.5V D-CDM voltage, most noticeable seen on 7 out of 10 of these heads. This voltage level was approximately 25% lower than the initial resistance degradation voltage of ~5V. Discharges of either Positive or Negative ESD events produced similar effects without noticeable distinction. We can say that the other 3 heads had no significant degradation of performance until catastrophic damage occured.

From the Transfer Curve analysis during the ESD sweep we can conclude that the most likely increase in MAN noise is as a result of the introduction of hard and soft kinks, often times very subtle. These kinks may be new features added by the ESD stress, or previously existing features that have been ‘shifted’ into the measurement range by the ESD, and this question must be studied further. Equally, existing kinks may be ‘shifted’ out of the normal operating range, making the head appear more sound than it should be.

We can also conclude that the amplitude measurement alone has limitations in ability to detect partial ESD damage due to D-CDM.

Lastly we can conclude that no additional instabilities appeared on these HGAs as a result of Write Stress, above and beyond the baseline MAN noise.

IX. Conclusion

In many cases heads that appear to be stable can become unstable by partial ESD damage. Amplitude alone may not be a good characterization tool for this condition, as it cannot always detect instabilities. Specific instability measurement tools, such as MAN, may be required to catch these cases.

References

1. L. Baril, M Nichols, and A. Wallash, "Degradation of GMR and TMR Recording Heads Using very short duration ESD Transients" *Intermag Europe 2002*.
2. M Nichols, "Noise And Discontinuities in GMR Transfer Curves" *Intermag Europe 2002*.